Simultaneous Continuous, Nonchromatographic Monitoring and Discrete Chromatographic Monitoring of Polymerization Reactions

Alina M. Alb, Michael F. Drenski, Wayne F. Reed

Tulane Center for Polymer Reaction Monitoring and Characterization (PolyRMC), Tulane University, New Orleans, Louisiana 70118

Received 7 August 2008; accepted 19 October 2008
DOI 10.1002/app.29501
Published online 16 March 2009 in Wiley InterScience (www.interscience.wiley.com).

ABSTRACT: Automatic continuous nonchromatographic monitoring and discrete chromatographic monitoring were coupled together for the first time and used to monitor free radical and controlled-radical polymerization reactions. This was achieved by adding a multidetector Size Exclusion Chromatography (SEC) system (alternatively termed Gel Permeation Chromatography, GPC) to the ACOMP platform (Automatic Continuous Online Monitoring of Polymerization reactions). The fact that the reactor solution is already preconditioned in the ACOMP front-end to the concentration levels used in SEC makes direct coupling possible. Kinetics from two different types of reactions, Reversible Addition Fragmentation Transfer (RAFT) and free radical polymerization of butyl acrylate were studied, including the production of a bimodal population. Complementary and contrasting features from the continuous and SEC approaches are highlighted. The main advantage of the SEC detection is to follow the evolution of full molecular weight distributions (MWD), especially in 'living' type reactions, where polydispersity decreases with monomer conversion, whereas the continuous detection provides a much more detailed characterization of the reaction. Interestingly, in the case where a bimodal molecular weight distribution was produced, the continuous method automatically detected the onset of the second mode in a model independent fashion, whereas SEC could only discern the bimodality by applying preconceived models. The SEC approach will have valuable niche applications, however, such as when reactions are relatively slow, monitoring narrow polydispersity is of primary importance, and also in copolymerization and terpolymerization reactions where complex mixtures of reagents (e.g., RAFT agents, copper ions, etc.) make unfractionated spectroscopic resolution of comonomers difficult.
 J Appl Polym Sci 113: 190–198, 2009

Key words: gel permeation chromatography (GPC); kinetics (polym.); light scattering; living polymerization; molecular weight distribution/molar

INTRODUCTION

Monitoring polymerization reactions online has many benefits. These include obtaining comprehensive, quantitative data for understanding fundamental mechanisms and kinetics, for optimizing reaction processes, and, ultimately, for precisely controlling reactions to yield desired products. Monitoring approaches are becoming increasingly important as the sophistication of polymer syntheses increases to include new approaches to creating precisely tailored, functional polymers with specific architectures. At the industrial level, such monitoring will allow for superior product consistency and quality and more efficient use of petroleum and other nonrenewable resources, plant and personnel time, and reduced greenhouse gas emissions per kilogram of product.

Of the many approaches to monitoring, this work concentrates on developments in the ACOMP area (Automatic Continuous Online Monitoring of Polymerization reactions). ACOMP is a rapidly developing, flexible method that obtains massive amounts of information rich data through an integrated platform.[1–3] Typically, the ACOMP detector train will furnish, at desired intervals, such as each second, hundreds of signals; e.g., light scattering from multiple scattering angles, viscometer, refractometer, temperature, pH, and conductivity signals, and multiple-wavelength UV/visible absorbance, and near infrared signals. Recently, Mie scattering data has also been added for monitoring emulsion polymerization reactions.[4] These many different types of signals can be combined in different ways to provide

Correspondence to: W. F. Reed (wreed@tulane.edu).
Contract grant sponsor: NSF; contract grant number: CBET 062531.
Contract grant sponsor: Louisiana Board of Regents; contract grant number: LEQSF(2007-10)-RD-B-05.
Contract grant sponsor: NASA; contract grant number: NCC3-946.
Contract grant sponsor: Tulane Institute for Macromolecular Engineering and Science, Tulane Center for Polymer Reaction Monitoring and Characterization (PolyRMC).

a comprehensive, and often model-independent characterization of polymerization and copolymerization reactions in terms of kinetics, monomer and co-monomer conversion, average composition drift and distribution, and the evolution of weight-average molecular weight M_w, and intrinsic viscosity $[\eta]_w$. Secondary, model-dependent quantities, such as reactivity ratios and sequence length distributions are frequently computed on the basis of the primary data.

Other methods for monitoring polymerization reactions include such *in situ* methods as Raman Spectroscopy, near infrared, and mid infrared.[5–15]

The object of this work is to expand the information-rich approach of ACOMP to include automatic multidetector Size Exclusion Chromatography (SEC) data simultaneously with the continuous nonchromatographic data usually collected in ACOMP. (SEC is often also termed Gel Permeation Chromatography, GPC). This is made possible because the ACOMP dilution levels and sample conditioning (e.g., debubbling) are the same as those used in SEC, so that the sample stream issuing from the continuous ACOMP detectors can be automatically and periodically injected into the SEC system. The strengths and weaknesses of each approach can then be addressed. To contrast different scenarios, both 'living' type RAFT reactions[16] and classical free radical polymerizations were carried out, including the production of bimodal molecular weight distributions (MWD). Butyl acrylate in butyl acetate was chosen for the study.

It is pointed out that a detailed SEC investigation, *per se*, of the polyacrylate products is not within the scope of this work, nor a study of the limits of SEC for polyacrylate analysis. Rather, the direct comparison of kinetic and molecular weight from the continuous nonchromatographic and SEC approaches is the focus. In fact, there are several excellent publications dealing with SEC and polyacrylates, including the issue of branching.[17–19]

EXPERIMENTAL

Materials and procedure

The RAFT agent, 2-{[(dodecylsulfanyl)carbonothioyl]sulfanyl} propanoic acid (DoPAT) (>99.5% purity), was supplied by Dr. Algirdas Serelis of Dulux Australia (Victoria, Australia). AIBN was used as the initiator. Butyl acrylate (BA), methyl methacrylate (MMA), butyl acetate, and AIBN were used as received from Sigma (>99% purity). Reactions were carried out with a total of 20–35% by mass BA in butyl acetate in a 100-mL three-neck reactor under N_2 blanket at 70°C. Table I summarizes the reactions reported here; RAFT homopolymerization of BA, free radical polymerization of BA at two different concentrations, and free radical of BA with 'booster' initiator.

TABLE I
Reaction Conditions for the Experiments

#	[M]	[I]	[DoPAT]
1	2.7	0.0167	0.00833
2	2.7	0.0167	–
3	2.0	0.0111	–
4	2.0	0.0033[a]	–

The reactions were done at 70°C.
[a] An initiator boost by 16× this value was made at $f = 0.45$.

ACOMP

ACOMP background, theory, and instrumentation have been described in detail previously.[1–4] The reactor liquid was purged with N_2 before and throughout the reaction and a small stream was withdrawn continuously at 0.1 mL/min by a Shimadzu HPLC (Columbia, MD) pump and further diluted with butyl acetate before reaching the detector train. A five-pump system was used so that the reactor solution is diluted in two stages, one (~ 7%) in a low pressure mixing chamber pressure, the other (10%) in a high pressure mixing chamber, yielding a 150 fold dilution. The total detector flow rate was 2.0 mL/min, yielding ~ 1.8–2.4 mg/mL of combined monomer/polymer concentration, depending on the experiment.

The ACOMP detector train was a typical one, and included a Brookhaven Instruments Corp (Holtsville, NY). BI-MwA seven angle scattering instrument (MALS), a Shimadzu RID-10A refractometer (RI), a custom-built single capillary viscometer, and a Shimadzu SM20 photodiode array UV/visible spectrophotometer (UV).

SEC

The waste stream of the ACOMP system was connected to a Rheodyne MXP 7900 injector valve with a 100-μL sample loop attached. An Amperite solid state DFA series adjustable recycling timer was used to control the valve for periodic injections, generally every 10 min. This recycling time can be adjusted to suit the elution time of the sample being injected. The goal is to maximize the number of injections made throughout the polymerization experiment while not adversely affecting the elution peak of the polymer.

The SEC flow rate was 1.0 mL/min. Following the injector, a standard SEC system was built, with columns provided by Polymer Laboratories (now a part of Varian, Walnut Creek, CA). In the case of RAFT polymerization a PLgel 5-μm column (pore size

500Å) was used, and a PLgel Mixed-B 10-μm column was used for free radical polymerization reactions. This approach of using a single standard SEC column was chosen as a compromise between a reasonable sampling frequency (every 10 min) and resolution. There is currently interest in 'fast SEC' and construction and evaluation of different column packing and geometries is ongoing. 'Fast SEC' still involves a trade-off between speed and resolution.[20,21] If the usual analytical approach of using two or more traditional columns to get a high level of separation and chromatographic resolution is used the sampling rate will generally be too slow for polymerization monitoring, except for extremely slow reactions (lasting many hours).

The SEC detector train was similar to that of the continuous nonchromatographic train described above, and comprised another BI-MwA MALS, Shimadzu RI and dual wavelength UV. The UV wavelength monitored was 250 nm. The SEC viscometer, however, was a custom-built bridge capillary viscometer utilizing a matched capillary bridge provided by Polymer Laboratories. Although this type of viscometer offers superior results in SEC applications, compared to single capillary viscometers, it is unsuitable for continuous monitoring, at least in its standard configurations, because the hold up volume (provided here by a chromatographic guard column) quickly saturates with monomer/polymer from the ACOMP stream.

Although an extensive comparison of single capillary and bridge capillary viscometers has been presented,[22] a few salient features are mentioned here. In general, the bridge viscometer will give superior signal/noise ratio, but requires two separately calibrated pressure transducers. In the case of the single-capillary viscometer, the reduced viscosity is independent of any calibration factors and is computed at each sampling point i, according to

$$\eta_{r,w,i} \equiv \frac{\eta_i - \eta_0}{\eta_0 c_i} = \frac{P_i - P_0}{P_0 c_i} = \frac{V_i - V_0}{V_0 c_i} \quad (1)$$

where P_i represents the pressure drop along the capillary and V_i represents the voltage signal corresponding to that drop, both at elution point i. P_0 and V_0 refer to the average solvent baseline values. Note that since the same transducer is used to measure all quantities in the expression, any calibration factors cancel out, so that no calibration is necessary. In contrast the computation of $\eta_{r,w,i}$ for the bridge viscometer, is

$$\eta_{sp,i} \equiv \frac{4P_{\Delta,i}}{(P_{B,i} - 2P_{\Delta,i})c_i} = \frac{4K_\Delta V_{\Delta,i}}{(K_B V_{B,i} - 2K_\Delta V_{\Delta,i})_i} \quad (2)$$

where P_Δ is the pressure difference between the two arms of the bridge, P_B is the pressure drop across the arms of the bridge, and K_Δ and K_B are the calibration constants needed to convert the voltage received from the two transducers into the respective pressure drops. In this work, the calibration constants were $K_\Delta = 1$ kPA/V, and $K_B = 20$ kPa/V.

Although MALS in the SEC detector train avoids traditional column calibration using polymer standards, in this work RI calibration curves were made with polystyrene (PS) standards, with molecular masses ranging from 1660 to 3.06×10^6 g/mol, depending on the type of the column used (Polymer Laboratories) to compare the MALS and column calibration results for molecular weights. The value of *dn/dc* for pBA in butyl acetate was determined using the RI detector to be 0.080.

It will be useful in the results analysis to have the following elution data for standards, and viscosity molecular weight relationships:

For the PL Gel 5-μm column, the PS standards in Butyl Acetate yielded, $M_p = 2.25 \times 10^7 \exp(-1.0849x)$, where x = elution volume in mL.

For the PLgel Mixed-B 10-μm column, the PS standards in Butyl Acetate yielded, $M_p = 1.416 \times 10^{12}\exp(-2.1311x)$, where x = elution volume in mL.

Using the differential viscometer values for the polystyrene standards in butyl acetate yielded the following relationship

$[\eta] = 0.023874M^{0.6070}$

Using the differential viscometer values for poly (butyl acrylate), or pBA, in butyl acetate yielded the following relationship

$[\eta] = 0.001987M^{0.8707}$

The quantity $M[\eta]$ is proportional to polymer hydrodynamic volume V_H. In the relevant polymer range of $M > 5000$ g/mol V_H for pBA is larger than the corresponding V_H value for PS at any given mass.

The analog signals from each of the detectors were collected with the BIMwA four channel A/D board and recorded with the BITDSLS software at 1 Hz.

RESULTS

RAFT and free radical polymerization reactions

Figure 1a shows continuous, nonchromatographic raw ACOMP signals from the different detectors for RAFT polymerization of BA (#1, Table I). The increase of light scattering at 90° (LS90) and viscometer (shown in the overlay) voltages follows the growth of the polymer chains, whereas the decrease in UV (the 245 nm data are shown, selected from the complete UV spectrum gathered) and increase in RI follows the monomer consumption. Temperature during the reaction was also monitored and is shown in the Figure 1(a) overlay.

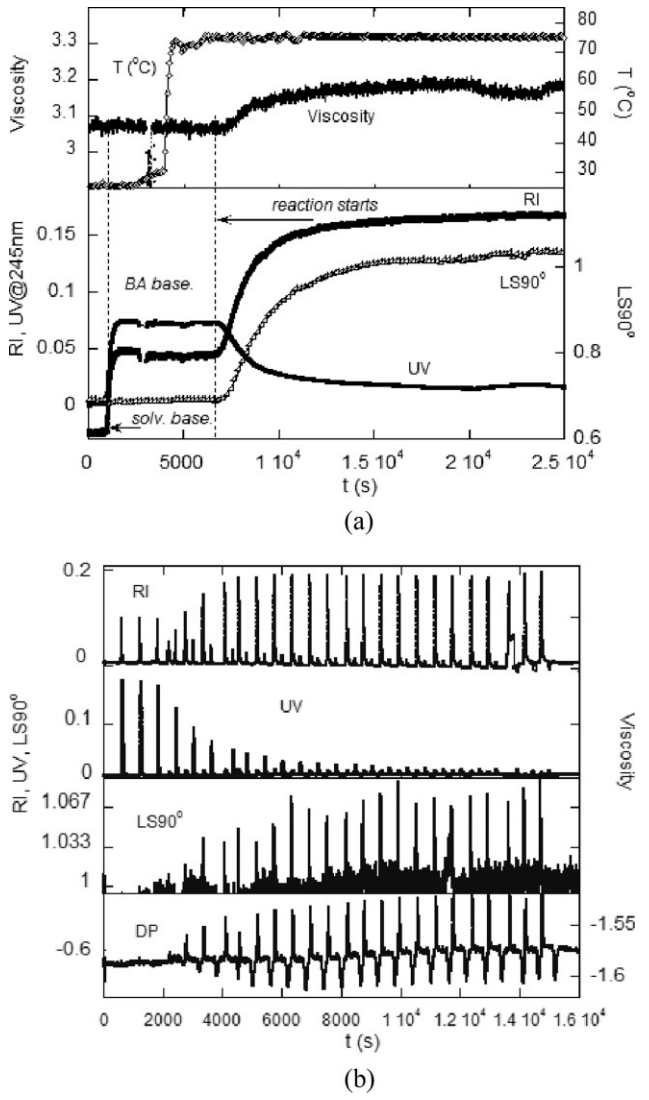

Figure 1 (a) Raw ACOMP signals for reaction #1. (b) Multidetector SEC signals obtained for reaction #1, obtained simultaneously with those of Figure 1(a).

Figure 1(b) shows raw SEC signals from the same reaction; RI, UV at 250 nm, light scattering at 90° (LS90), and differential viscometer pressure (DP). The evolution of RI, UV at 250 nm, and LS90 follows the kinetics of the reaction monitored by ACOMP. The interval between injections was 10 min. The negative pulses in the DP data are due to the elution of the split pulse of the fractionated mass that went through the arm in the capillary bridge where the hold-up volume was located. As the hold up volume in this case was an SEC guard column, the pulse of material is essentially maintained, though somewhat broadened, and gives a negative pulse when it finally leaves the capillary with the hold-up volume. If the guard column used for hold-up volume is replaced by a simple empty volume, e.g., an unpacked column, the negative pulse is eliminated.

Figure 2 shows fractional monomer conversion f, versus time for the BA free radical and RAFT reactions (#1 and #2 in Table I), as obtained from the combined RI and UV (at 245 nm) signals. As expected,[23] the reaction rates depends almost entirely on the initiator concentration and are not affected by the presence of the RAFT agent, used in the case of the controlled reaction. Shown in the inset are light scattering signatures as functions of the monomer conversion for the initial portions of the same reactions. The formation of large polymer chains in the case of the free radical polymerization reaction is indicated by the high light scattering values observed. Contrasting LS behavior is shown for the reaction done in a controlled fashion (RAFT).

For free radical polymerization M_w often decreases linearly in time as $M_w = M_{w,0}(1 - \varepsilon f)$, where $\varepsilon = 1/2$ when there is no chain transfer at all, and initiator lifetime is long compared to the reaction time, and $\varepsilon = 0$ when there is strong chain transfer to monomer. With this, for free radical polymerization

$$I(f) = Kc_{m,0}M_{w,0}(1 - \varepsilon f)f \tag{3}$$

where $c_{m,0}$ is initial monomer concentration in detector chain, K is the usual optical constant for light scattering of vertically polarized incident light, and $M_{w,0}$ is the initial M_w of the reaction.

Likewise, for 'living' reactions, I(f) is parabolic,

$$I(f) = Kc_{m,0}M_{\text{final}}f^2 \tag{4}$$

and M_{final} is the final target mass of the living polymerization. The fits to the LS data in the inset of

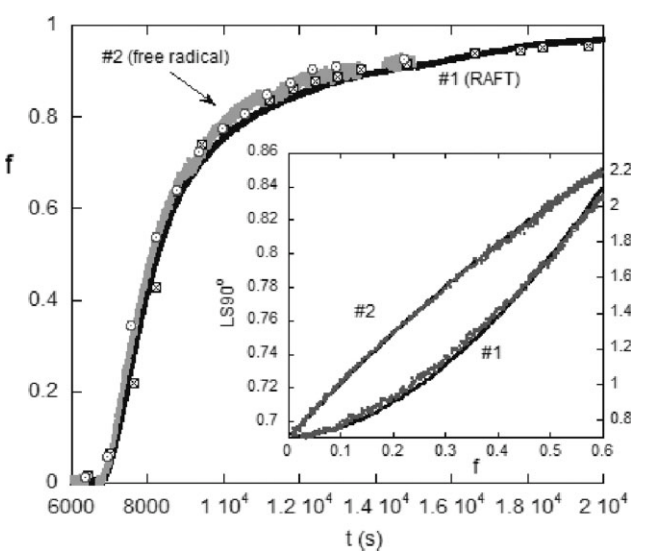

Figure 2 Fractional monomer conversion f versus t for RAFT (reaction #1) and free radical BA polymerization (reaction #2). The inset shows the raw light scattering (LS90) signal versus f, together with fits to the predicted behavior for each type of reaction [eqs. (3) and (4)].

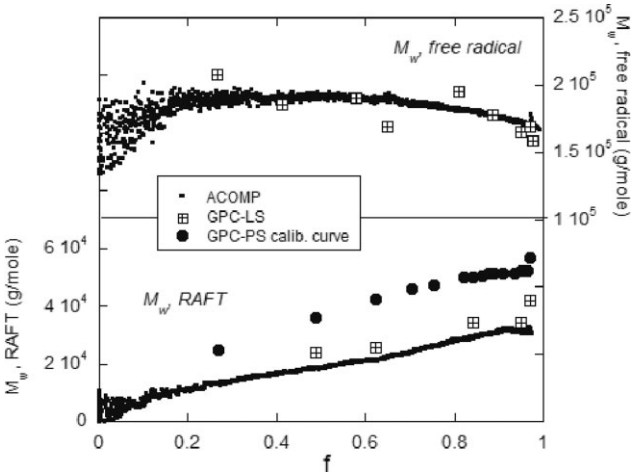

Figure 3 M_w versus f for 'living' RAFT reaction #1 (lower pane) and for free radical reaction #3 (upper pane). Also shown are values from the automatic SEC-MALS data. For the RAFT data the discrete circles show the equivalent molecular weights obtained by calibration of the column by polystyrene standards.

Figure 2 are according to eqs. (1) and (2), and show how the free radical and controlled radical nature of reactions #2 and #1, respectively, are evident directly from the raw LS data.

Figure 3 shows the evolution of weight average molecular weight M_w with conversion for reactions #1 (bottom pane) and #3 (top pane). M_w was obtained using the well known Zimm equation[24] according to previously established ACOMP procedures.[1–3] This involves combining the polymer concentration obtained from f with the light scattering data extrapolated to zero angle, and with a small correction due to the second virial coefficient A_2. High molecular weight polymer is observed in the free radical polymerization reaction, with little change in its value, while in the case of the RAFT reaction, polymer mass grows gradually, in a linear fashion, as expected for a 'living' type reaction.

It is important to point out that branching has been detected in the polymerization of acrylates.[25,17] The effects on reaction kinetics of intramolecular transfer to polymer,[26,27] likely backbiting,[28] and of intermolecular transfer to polymer have been studied. Long-chain branching is known to change the conformation of polymer molecules in solution and is thus of importance for the interpretation of the SEC results.[29,19] This group has also found evidence of branching for pBA reactions, where M_w versus conversion actually increased, rather than decreasing or remaining constant as is usual for free radical polymerization without branching.[2] In this work, however, there is no strong evidence of branching in the free radical reactions #2–#4. Deviations from first order monomer conversion are normally predicted when branching occurs,[17] but Figure 2 shows that conversion kinetics are quite first order for both the RAFT and free radical reactions. Data below on reaction #4 also indicate first order kinetics before and after the sudden increase in initiator.

Also shown in Figure 3 are the SEC points computed by multiangle scattering, for both reactions #1 and #3. An important observation from reaction #1 is that, because the masses start very small and increase linearly with conversion (living reaction), it was not until around 50% conversion that any usable light scattering data from the SEC could be obtained. In contrast, as is seen in Figure 1(a), the continuous ACOMP detectors begin to furnish good light scattering data as soon as conversion begins, yielding the good, continuous M_w data in the bottom curve of Figure 3. For the free radical polymerization, large polymer was produced from the start, and by about 25% conversion there was enough polymer concentration that light scattering in the SEC data yielded meaningful M_w values. Again, however, the continuous ACOMP signals furnish a continuous record of M_w from the beginning of conversion.

Finally, as regards Figure 3, the molecular weights, obtained by calibration with PS standards, sometimes referred to as 'Polystyrene equivalent molecular weights' are shown for reaction #1. These give values far in excess of the absolute values computed by light scattering, using both the continuous and SEC data. Similar, erroneous results were found for the other reactions (PS equivalent data values not shown for the other experiments). This reinforces the well known fact that using standards for molecular weight calibration gives only the 'equivalent molecular weight' referenced to the particular standard polymer used, and not an absolute value. It is noted that computation of M_w via light scattering in SEC of the PS standards themselves led to values within 2% or less of the nominal values provided by the manufacturer (Polymer Laboratories). The reason that the PS equivalent values for pBA are overestimated is because, as shown in the viscosity/molecular weight relationships at the end of the Experimental section, the hydrodynamic value V_H, of pBA is greater for any given mass than for PS, and hence, for any given mass, the pBA will elute at lower elution volume, and be erroneously compared to a higher molecular weight PS. The PS equivalent values were corrected using the viscosity/molecular weight relationships at the end of the Experimental section; i.e., taking $V_H \propto [\eta]_{PS} M_{PS} = [\eta]_{pBA} M_{pBA}$. The results (not shown) are closer to those obtained by light scattering SEC and ACOMP but still not in full agreement.

The SEC data can furnish full MWD, which ACOMP cannot. Thus, SEC can be particularly useful for 'living' reactions, where obtaining low

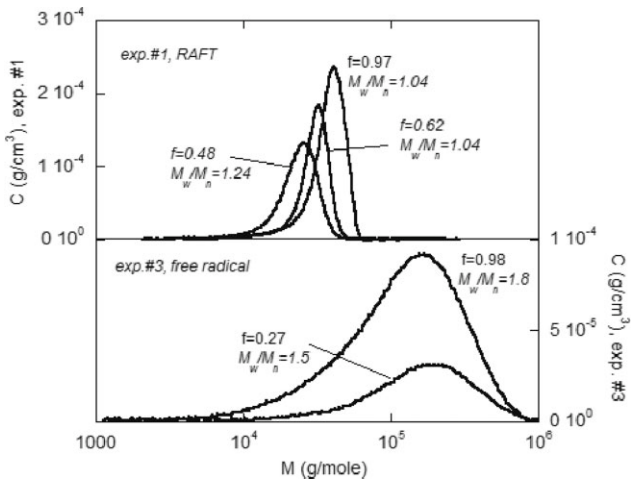

Figure 4 Molecular weight distributions (concentration versus M) at early, mid and late conversion in the RAFT (upper panel) and free radical (lower panel) reactions at early and late conversion, with the polydispersity index values, M_w/M_n, on the graph. The narrowness of the RAFT distributions contrast sharply with the broad distributions obtained by the free radical reaction.

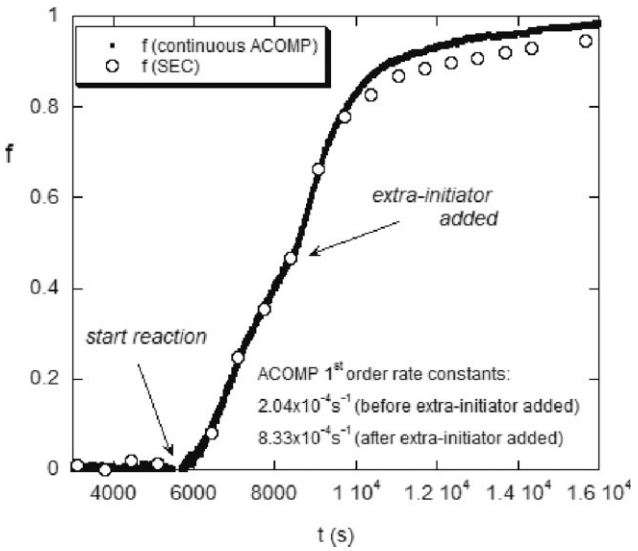

Figure 5 Monomer conversion f versus t for reaction #4 where an initiator boost was made at $f = 0.45$. Data obtained from both continuous and SEC (discrete circles) are shown. First order rate constants for the preboost and postboost portions of the reaction are also shown.

polydispersity is often a primary concern, and which are often slow enough to be able to gather SEC data. Figure 4 (earlier) shows how M_w/M_n decreases from 1.24 to 1.04 from early to mid-conversion and then stays about the same for the rest of conversion. The contrast with free radical reaction #3 (lower panel in Fig. 4) is striking. For these, the distribution starts quite broad, $M_w/M_n = 1.5$ and broadens to 1.8 by late in the reaction.

Bimodal molecular weight distributions in free radical reactions

Frequently, extra initiator is added during free radical reactions, sometimes to ensure reaction completion or to 'scavenge' residual monomers. Such initiator 'boosts' can also produce bimodality in the molecular weight distribution, if the initiator is added at early or intermediate levels of conversion.[30]

In reaction #4, an AIBN initiator boost of 16 times the initial AIBN concentration was given at monomer conversion $f = 0.45$. Figure 5 shows f versus t for this reaction. The very detailed, continuous data clearly show the increase in conversion rate after the boost. If the preboost and postboost conversion data are each fit with a single first order (exponential) the rates are 2.04×10^{-4} s^{-1} and 8.33×10^{-4} s^{-1}, respectively, which is in remarkable agreement with the Quasi Steady State Approximation[31] (QSSA) in the limit of slow initiator composition, for which the first order rate constant is predicted to be proportional to the square root of the initiator concentration.

Also shown in Figure 5 are f versus t points obtained from the automatic SEC data, using the UV signal at 250 nm in the SEC detection train. Although the SEC points closely follow the continuous data, the number of points is much smaller and the change in the kinetics could possibly be overlooked. Hence, the continuous data produces superior results for quantifying detailed conversion.

Figure 6 shows the effect of the initiator boost on M_w, which displays a rapid change in slope at the moment the initiator is added. M_w as measured by ACOMP is the cumulative value in the reactor. The instantaneous weight average molecular weight

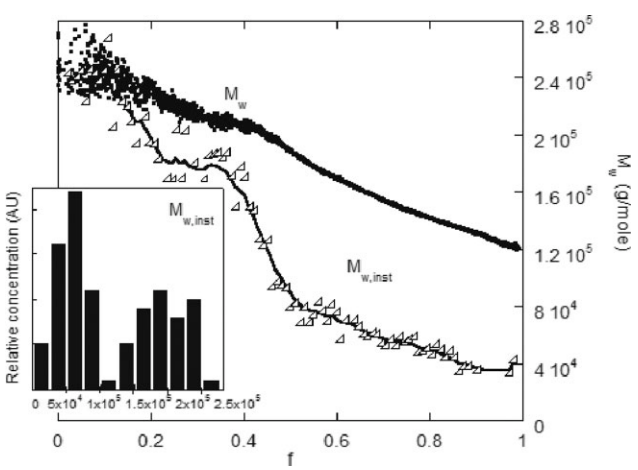

Figure 6 M_w versus f for reaction #4, and $M_{w,\mathrm{inst}}$, computed according to eq. (5). The inset shows a histogram of the mass distribution from this continuous data, where the bimodality is striking.

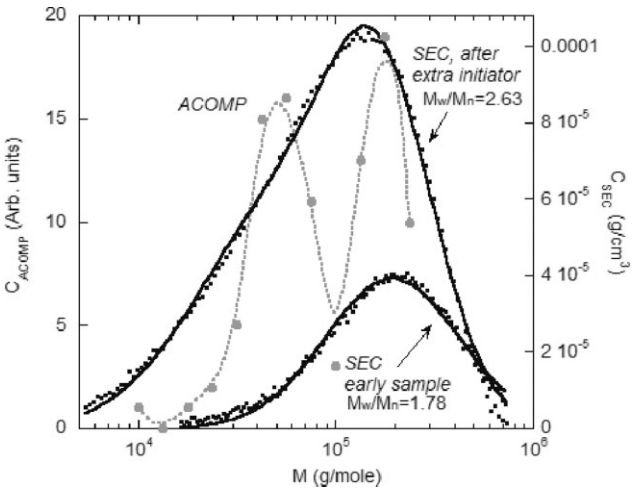

Figure 7 Molecular weight distributions for early and late conversion of free radical reaction #4, with initiator boost, together with log-normal fits. The dotted line shows the logarithmically binned $M_{w,\text{inst}}$ data from ACOMP, which clearly reveals the bimodality of the molecular weight distribution, which the SEC data does not directly show.

$M_{w,\text{inst}}$ can be computed from the cumulative data via

$$M_{w,\text{inst}} = \frac{d(fM_w)}{df} \tag{5}$$

$M_{w,\text{inst}}$ is also shown in Figure 6, and the abrupt drop is seen when the initiator is added. There is hence a bimodal population produced, with the first mode centered around $M_{w,\text{inst}} = 190{,}000$ and the second around $M_{w,\text{inst}} = 50{,}000$. This bimodality is detected directly from the ACOMP data without recourse to any model. ($M_{w,\text{inst}}$ follows by mathematical necessity from cumulative M_w and is not model-dependent).

The inset to Figure 6 shows a histogram of $M_{w,\text{inst}}$ from sorting the $M_{w,\text{inst}}$ data in Figure 6 into 'bins'. The bimodality is clearly seen, again without making any *a priori* assumptions about the nature of the distribution. The ratio of the mean masses of about four is also in agreement with the QSSA for free radical polymerization kinetics, where, for a given monomer concentration and in the absence of significant chain transfer, the kinetic chain length varies as the inverse square of the initiator concentration.

In contrast, the SEC data in Figure 7 show a very significant broadening of the MWD, but there is no apparent bimodality. Addition of one or more extra SEC columns to enhance resolution could make the bimodality more apparent, but at the expense of slowing the SEC sampling frequency; e.g., one extra column halves the sampling frequency and two extra columns cuts it to one third. As it is, using the single column, the following analysis can be made. Because it is known, *a priori*, that a bimodal MWD will result from the initiator boost, it is possible to invoke a preconceived model in which the net chromatogram is assumed to be the superposition of two single modes, each of which is best fit by a log-normal distribution. The result of a single log-normal fit to the early (preboost) MWD is shown in the figure, along with a double log-normal fit to an MWD toward the end of the reaction. The latter fit is good, which corroborates the assumption of the bimodal distribution, but the bimodal assumption has first to be made, and is not an immediate consequence of the direct SEC MWD analysis. The fit to the SEC MWD places the peaks of the bimodal distribution at 180,000 and 57,000, fairly close to the factor of four predicted, and close to the ACOMP values. It should also be pointed out that this separation in peak masses is not strong, so that even multiple columns might fail to clearly reveal the bimodality.

The dotted line MWD in Figure 7 is that obtained from the continuous ACOMP data, by 'binning' the $M_{w,\text{inst}}$ data logarithmically. Again, the bimodality is very clear via continuous detection.

Finally, as regards the initiator boost reaction, Figure 8a shows how the continuous viscosity data also reveals the bimodality. The viscosity measurements are independent of the light scattering measurements, so this is a good cross-check on the result. Under the low polymer concentration conditions in the detector, the weight average reduced viscosity computed directly from the single capillary viscosity data is very close to the weight average intrinsic viscosity $[\eta]_w$, and is hence represented as such in Figure 8(a). The continuous data show the decrease in $[\eta]_w$. The bimodality is made striking in Figure 8(a), however, by computing the instantaneous weight average intrinsic viscosity $[\eta]_w$ via,

$$[\eta]_{w,\text{inst}} = \frac{d(f[\eta]_w)}{df} \tag{6}$$

The values of $[\eta]_w$ in Figure 8(a) obtained from the differential viscometer on the SEC detector train, shown by the discrete crosses, are in reasonable agreement with those obtained by the continuous data from the single capillary viscometer. Again, although the concentration of polymer entering the continuous detectors and SEC trains are the same, the material passing through the SEC columns gets highly diluted and may hence often yield noisier data than the corresponding continuous measurement, and it is hard to obtain reliable viscosity and light scattering data at early conversion points.

Figure 8(b) plots log[η] versus Log(M) for the last automatic SEC injection from the bimodal experiment. A relationship of $[\eta] = 0.001987M^{0.8707}$ is

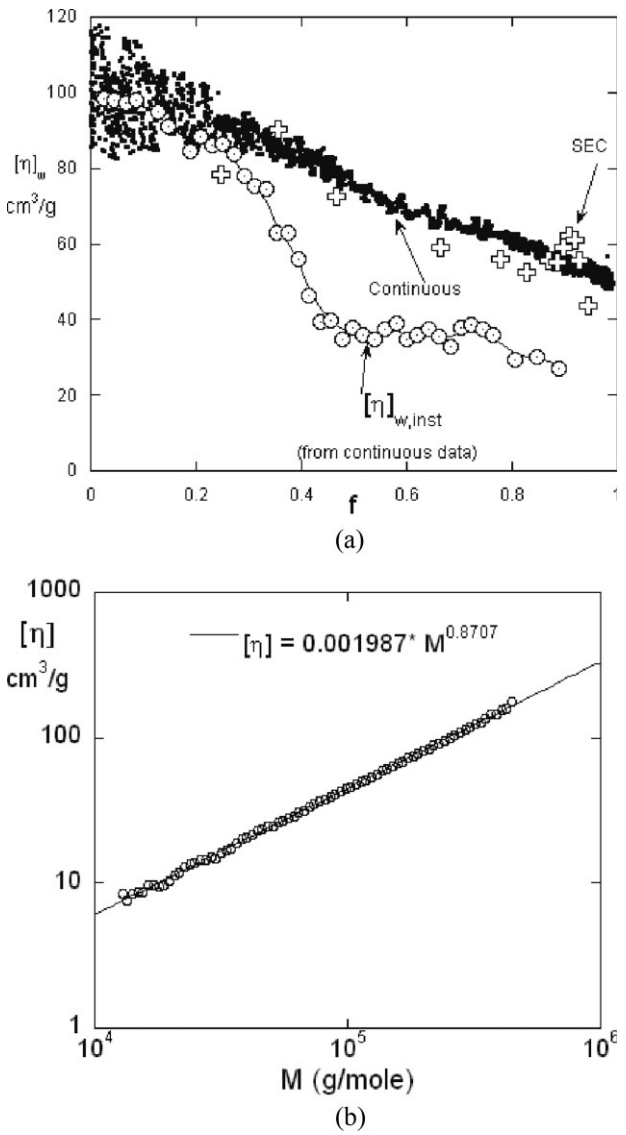

Figure 8 (a) $[\eta]_w$ versus f for the initiator boost reaction (#4). Also shown is $[\eta]_{w,inst}$, obtained from the continuous data via eq. (6), which clearly shows the bimodality. The corresponding discrete $[\eta]_w$ points from the SEC differential viscometer are also shown. (b) log[η] versus log(M), and the associated power law fit, from the last automatic SEC aliquot from reaction #4.

obtained, which was the source of this expression given at the end of the Experimental section. The exponent is close to the typical value of 0.8 for linear polymer chains in a good solvent (i.e., with strong excluded volume). The excellent linearity spans nearly two orders of magnitude in M, and shows that, despite the bimodality, the architecture of the shorter polymer chains produced after the initiator boost do not differ at all from the larger chains produced at the outset. It is recalled that the viscosity exponent in these relations is particularly sensitive to small errors in interdetector dead volume, since three detectors are used in the computation (MALS, viscosity, and UV or RI).[32] Computation of M is also sensitive to dead volume, but involves only two detectors (MALS and UV or RI). In any case, the average values of M_w and $[\eta]_w$ from SEC result from ratios of the separately integrated detector peaks, and are, hence, independent of dead volume.

CONCLUSIONS

Addition of multidetector SEC enhances the already massive data gathering power of ACOMP. The most valuable complementary information obtained by the SEC is the full molecular weight distribution that can be obtained, as opposed to the average values M_w and $M_{w,inst}$, and the average distribution that the latter offers, which are obtained by continuous, nonchromatographic detection.

The ability of the SEC approach to furnish meaningful molecular weight distributions will depend both on the details of the reaction and which column(s) are used; Obviously, short columns for rapid SEC will increase frequency of data points but degrade resolution, while adding multiple columns can enhance resolution but seriously diminish the frequency of data points. In the current work a single, conventional size analytical column was not able to directly resolve a narrowly separated bimodal distribution, but the resulting broadened distribution could be resolved into bimodal components with a model dependent assumption.

Ironically, in the initiator boost reaction here, the continuous, nonchromatographic approach was able clearly to detect the onset of MWD bimodality without any model assumptions, in all its detectors and quantities; conversion, M_w, and $[\eta]_w$, whereas the SEC detection, with only a single column, could not directly detect the bimodality. Addition of extra columns could improve resolution, but at the expense of SEC sampling frequency.

Although continuous detection in ACOMP can reveal bimodalities and population broadening for free radical reactions, eqs. (5) and (6) do not apply for living reactions, so that ACOMP-SEC will be important for determining polydispersity in living reactions, while the continuous detectors will give much better and more detailed data on monomer conversion and the evolution of M_w and $[\eta]_w$. ACOMP-SEC will also be well suited for living reactions that are slow, so that more data points per unit of conversion can be obtained.

Using small pore columns, the SEC approach will probably be useful in copolymerization, and possibly terpolymerization, for monitoring the conversion of comonomers[33] when other spectroscopically interfering agents are used in the reaction, such as RAFT agents, copper ions, etc.

Not unexpectedly, use of column calibration via polymer standards (polystyrene standards in this case), lead to results dramatically different than the absolute values furnished by light scattering, in both the continuous and SEC/light scattering data. As a practical matter, it can be very useful to have both SEC detection and continuous detection, but where the expense of a complete multidetector SEC system would be prohibitive, a simple concentration detector (e.g., RI or UV) equipped SEC stage could be used, and the column calibrated to the materials produced, to estimate polydispersity from the single concentration detector.

References

1. Florenzano, F. H.; Strelitzki, R.; Reed, W. F. Macromolecules 1998, 31, 7226.
2. Alb, A. M.; Enohnyaket, P.; Drenski, M. F.; Head, A.; Reed, A. W.; Reed, W. F. Macromolecules 2006, 39, 5705.
3. Alb, A. M.; Drenski, M. F.; Reed, W. F. Polym Int 2008, 57, 390.
4. Alb, A. M.; Reed, W. F. Macromolecules 2008, 41, 2406.
5. Van den Brink, M.; Pepers, M.; Van Herk, A. M.; German, A. L. Polym React Eng 2001, 9, 101.
6. Long, T. E.; Liu, H. Y.; Schell, B. A.; Teegarden, D. M.; Uerz, D. S. Macromolecules 1993, 26, 6237.
7. Vieira, R.; Sayer, C.; Lima, E.; Pinto, J. J Appl Polym Sci 2002, 84, 2670.
8. Fontoura, J M. R.; Santos, A. F.; Silva, F. M.; Lenzi, M. K.; Lima, E. L.; Pinto J. C. J Appl Polym Sci 2003, 90, 1273.
9. Reis, M. M.; Araujo, P. H. H.; Sayer, C.; Giudici, R. Ind Eng Chem Res 2004, 43, 7243.
10. Storey, R. F.; Donnalley, A. B.; Maggio, T. L. Macromolecules 1998, 31, 1523.
11. Reshadat, R.; Balke, S. T. Appl Spectrosc 1999, 53, 1309.
12. Hill, D. J. T.; Shao, L. Y.; Pomery, P. J.; Whittaker, A. K. Polymer 2001, 42, 4791.
13. Cardenas-Valencia, A. M.; Shastry, V.; Garcia-Rubio, L. H., In Situ Spectroscopy of Monomer and Polymer Synthesis; Puskas, J. E.; Long, T. E.; Storey, R. F., Eds.; ACS Symp; American Chemical Society: Washington, D.C., 2003, p 83.
14. Elizalde, O.; Asua, J. M.; Leiza, J. R. Appl Spectrosc 2005, 59, 1270.
15. Stavropoulos, Y.; Kammona, O.; Chatzi, E. G.; Kiparissides, C. J Appl Polym Sci 2001, 82, 1776.
16. Chiefari, J.; Chong, Y. K.; Ercole, F.; Krstina, J.; Jeffery, J.; Le, T. P. T.; Mayadunne, R. T. A.; Meijs, G. F.; Moad, C. L.; Moad, G.; Rizzardo, E.; Thang, S. H. Macromolecules 1998, 31, 5559.
17. Plessis, C.; Arzamendi, G.; Leiza, J. R.; Alberdi, J. M.; Schoonbrood, H. A. S.; Charmot, D.; Asua, J. M. J. Polym Sci Polym Chem 2001, 39, 1106.
18. Asua, J. M.; Beuermann, S.; Buback, M.; Castignolles, P.; Charleux, B.; Gilbert, R. G.; Hutchinson, R. A.; Leiza, J. R.; Nikitin, A. N.; Vairon, J. P.; van Herk, A. M. Macromol Chem Phys 2004, 205, 2151.
19. Gaborieau, M.; Nicolas, J.; Save, M.; Charleux, B.; Vairon, J.-P; Gilbert, R. G; Castignolles, P. J Chromatogr A 2008, 1190, 215.
20. Pasch, H.; Kilz, P. Macromol Rapid Commun 2003, 24, 104.
21. Popovici, S. T.; Schoenmakers, P. J. J Chromatogr A 2005, 1099, 92.
22. Norwood, D. P.; Reed, W. F. Int J Polym Ana Char 1997, 4, 99.
23. Alb, A. M.; Serelis, A. K.; Reed, W. F. Macromolecules 2008, 41, 332.
24. Zimm, B. H. 16:1093 1948.
25. Ahmad, N. M.; Heatley, F.; Lovell, P. A. Macromolecules 1998, 31, 2822.
26. Nikitin, A. N.; Hutchinson, R. A. Macromolecules 2005, 38, 1581.
27. Nikitin, A. N.; Hutchinson, R. A.; Buback, M.; Hesse, P. Macromolecules 2007, 40, 8631.
28. Nikitin, A. N.; Castignolles, P.; Charleux, B.; Vairon, J P. Macromol Rapid Commun 2003, 24, 778.
29. Kostanski, L. K.; Keller, D. M.; Hamielec, A. E. J Biochem Biophys Methods 2004, 58, 159.
30. Reed, W. F. Macromolecules 2000, 33, 7165.
31. Dotson, N. A.; Galvan, R.; Laurence, R. L.; Tirrell, M. Polymerization Process Modeling; VCH Publishers: New York City, 1996.
32. Reed, W. F. Macromol Chem Phys 1995, 196, 1539.
33. Alb, A. M.; Enohnyaket, P.; Shunmugam, R.; Tew, G. N.; Reed, W. F. Macromolecules 2006, 39, 8283.